Optics Communications 366 (2016) 94–98

Contents lists available at ScienceDirect

Optics Communications

journal homepage: www.elsevier.com/locate/optcom

Invited Paper

Rolling Shutter Effect aberration compensation in Digital Holographic Microscopy

Andrea C. Monaldi [a,b,*], Gladis G. Romero [a,b], Carlos M. Cabrera [a], Adriana V. Blanc [a,b], Elvio E. Alanís [a]

[a] Universidad Nacional de Salta, Fac. de Cs. Exactas, Grupo de Óptica Láser, Av. Bolivia 5150, 4400 Salta, Argentina
[b] INENCO–CONICET, Av. Bolivia 5150, 4400 Salta, Argentina

ARTICLE INFO

Article history:
Received 27 October 2014
Received in revised form
11 December 2015
Accepted 18 December 2015

Keywords:
CMOS
Digital Holographic Microscopy
Rolling Shutter Effect
Optical phase aberration

ABSTRACT

Due to the sequential-readout nature of most CMOS sensors, each row of the sensor array is exposed at a different time, resulting in the so-called rolling shutter effect that induces geometric distortion to the image if the video camera or the object moves during image acquisition. Particularly in digital holograms recording, while the sensor captures progressively each row of the hologram, interferometric fringes can oscillate due to external vibrations and/or noises even when the object under study remains motionless. The sensor records each hologram row in different instants of these disturbances. As a final effect, phase information is corrupted, distorting the reconstructed holograms quality. We present a fast and simple method for compensating this effect based on image processing tools. The method is exemplified by holograms of microscopic biological static objects. Results encourage incorporating CMOS sensors over CCD in Digital Holographic Microscopy due to a better resolution and less expensive benefits.

1. Introduction

A CCD/CMOS used to record holograms must resolve the interference pattern resulting from superposition of the reference wave with the waves scattered from different object points. In the last decades, in order to achieve digital holograms, CCD sensors have been chosen as the favorite ones for replacing the classical holographic films [1]. This is due to its ability to meet the minimum resolution requirements despite of its high cost. CMOS sensors have many advantages in comparison to the CCD sensors; they offer higher resolution, less thermal noise and guarantee higher frame rates at a significantly reduced cost compared to the CCD ones. Moreover, the main difference between CMOS and CCD sensors lies in the signal readout mechanism. To obtain signals corresponding to an image frame all photodiodes of CCD are exposed to a scene simultaneously; whereas, in most CMOS sensors each image row, being sequentially accessed, is given a different exposure time window, with a time delay defined by the sensor technology. Even though this readout mechanism has the advantage of minimizing buffer memory, it produces the so-called Rolling Shutter Effect (RSE) that distorts images of moving objects [2–4]. In this regard, it may represent a major obstacle in interferometry techniques. Although the aim of this paper is not an exhaustive study of how one type of device differs from another, we will focus on some properties that are sensitive to a particular application such as the Digital Holographic Microscopy (DHM) [1,5–9]. In the literature, several works report solutions for eliminating or mitigating RSE by using either mechanical or electrical devices or by mathematical algorithms that generally require multiple images of the same scene for synchronization [2,10]. These correction mechanisms are typically used in automatic vision devices or popular used cameras. Nevertheless, to our knowledge, methods for eliminating this effect for the case of images of digital holograms have not been developed yet.

During hologram recording, interference fringes are strongly sensitive to external noises, vibrations, etc.; causing spurious perturbations during the readout process which result in unwanted phase aberrations. These perturbations may vary in an unpredictable way from one acquisition to another because they depend on random external conditions, which are difficult to control. Since in many DHM applications accurate phase values must be extracted from the quantitative phase map [11], this aberration must be compensated in order to have access to reliable local information of the integrated optical path length (OPL) which can be used to measure either the integral refractive index or the topography of the object under study.

To overcome this drawback when using a CMOS as a recording device in DHM, a simple and fast methodology is proposed. It consists of a sequential application of image processing tools to

* Corresponding author at: Universidad Nacional de Salta, Fac. de Cs. Exactas, Grupo de Óptica Láser, Av. Bolivia 5150, 4400 Salta, Argentina.
E-mail address: acmonaldi@gmail.com (A.C. Monaldi).

http://dx.doi.org/10.1016/j.optcom.2015.12.048
0030-4018/

the continuous phase maps obtained from holograms of biological static objects. Experiments in holograms of uniform refractive index objects in non-vibration isolated environment have been conducted to quantify phase errors introduced by RSE. The numerical results of these experiments show that spurious phase variations introduced by RSE affect the true values of phase above the typical expected errors.

2. Overview of Digital Holographic Microscopy

The transmission DHM and phase image reconstruction techniques used for the present study have been described in Refs. 5, 6, and 7. Briefly, they consist of recording a hologram by means of interferometric set-up, onto a solid-state array detector such as a CCD or CMOS sensor and, subsequently, numerically reconstructing the information by means of a computer. A layout of digital holographic microscope prototype constructed for this purpose, is depicted in Fig. 1(a). Essentially, it is a Mach–Zehnder interferometer, whose object arm is fitted with a small microscope built by inserting an *X*–*Y* microscope stage to locate the sample and a microscope objective (MO) which acts as a magnifying lens and forms a real image of the object of interest. A TV camera, with a CMOS Bayer Array 2592×1944 pix^2, 1.75 μm square pixels, 8 bit deep and a frame rate up to 25 Hz is used to record digital holograms.

The reconstruction of the original microscopic field of view of the sample is performed digitally on a computer. This procedure simulates the reconstruction process in conventional holography, which consists of illuminating the hologram with a replica of the reference beam used in the registration stage. In this application, the reconstruction of holograms is carried out by using the angular spectrum propagation method [12]. As a result, an amplitude contrast image and a quantitative phase image are obtained. Illustratively in Fig. 2(a) hologram of a *Ceratium hirundinella* cell and the corresponding amplitude and phase images are shown.

3. Rolling Shutter Effect phase aberrations

To illustrate the unwanted phase aberration introduced by RSE we will focus our attention on Fig. 2(c). It is a two-dimensional phase distribution called the unwrapped phase image. As it can be seen, the image background is not uniform as it should be according to the homogeneity of the surrounding medium, in this case water. Thus, RSE shows up revealing itself as spurious horizontal ripples.

Usually, in DHM phase errors are quantified by computing the standard deviation (STD) noise level in a flat area of the unwrapped phase map [9,13]. In our case, this corresponds to the background of the image of Fig. 2(c). However, as it was emphasized, any background area is corrupted by horizontal ripples. To illustrate the influence of phase noise introduced by the RSE, phase values of profiles in the *X* (test rows in Fig. 2(c)) and *Y* (test column in Fig. 2(c)) directions corresponding to the background region in the unwrapped phase image are shown in Fig. 3.

In Fig. 3(a) both background *X* profiles (test row 1 and test row 2) have similar STD but have their phase mean average values differing in about 2 rad, which makes quantitatively evident RSE. In addition, by observing these graphs, it is noticed that phase values of the background deviate from a constant and that the deviation is much more significant in the vertical direction (Fig. 3 (b)) than in the horizontal one, as evidenced from the scale of the graphics. According to this fact, in this paper we assume that the STD of the *X*-profiles gives a measure of experimental phase noise level not related with RSE. In a similar way, the STD of the Y profiles is a measure of the phase aberration introduced by the RSE.

The STD of various profiles analyzed, yield an average value of 0.16 in the *X* direction, and 0.54 in the *Y* direction. In terms of optical path length, these values represent an average phase error of approximately 16 nm and 54 nm respectively.

Horizontal nature of the background image ripples in Fig. 2(c), identified as phase aberrations introduced by the RSE, suggests that proper spatial filtering in the unwrapped phase spectrum could eliminate it. This procedure has some drawbacks when trying to automate the process, due to the randomness of the phenomenon. An alternative to avoid frequency filtering consists in removing the information of the aberration directly from the phase maps. This is accomplished by identifying and removing spurious phase values with image processing tools as explained bellow.

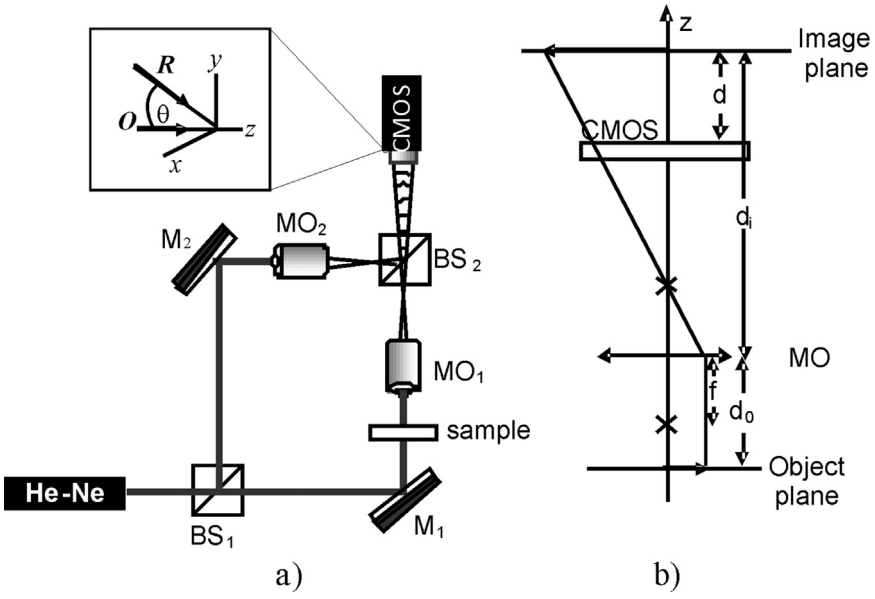

Fig. 1. : a) Experimental configuration; BS, beam splitters; M, mirrors; MO, microscope objectives. Inset: R, reference beam; O, object beam. b) Details of the microscope configuration in the object arm: d_0, object distance; d_i, image distance; f, MO focal length; d, distance of the image relative to the CMOS sensor.

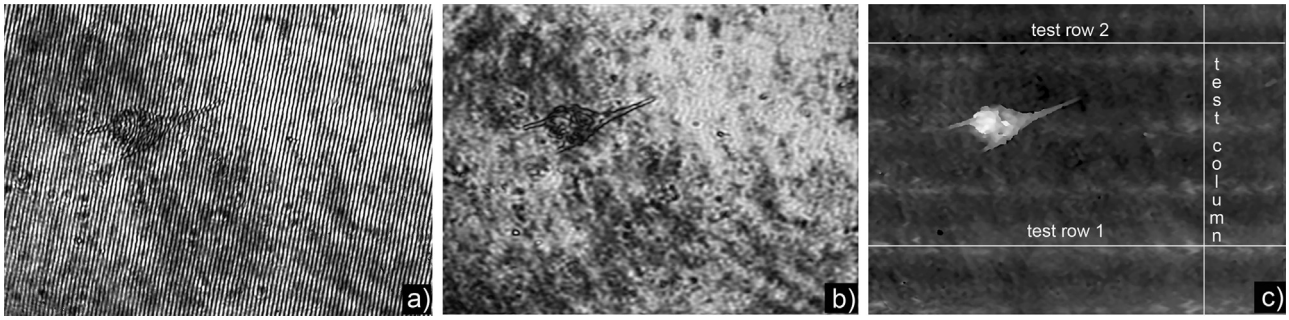

Fig. 2. : a) Hologram, b) Amplitude contrast image, c) Unwrapped phase.

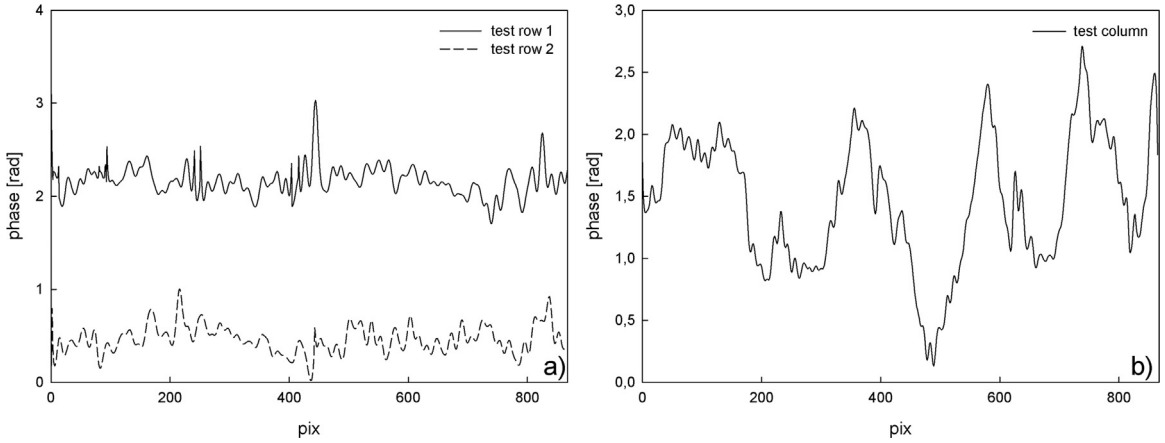

Fig. 3. Profiles of unwrapped phase image, a) *X*-profiles and b) *Y*-profile.

In absence of RSE, both background test rows of Fig. 3(a) should have similar median values. Thereby, when RSE is present, each row of the image has a different median value, which suggests that the median of each background row could be a representative phase value associated with the RSE. Based on this idea, our methodology for compensating the aberration consists of applying a sequential set of mathematical operations to the unwrapped *NXM* phase data matrix, which are summarized in the following.

The first step is calculating the median for the background pixels of each row (excluding all phase values of the object under study). All the medians of each row are stored in an *Nx1* array and a Gaussian filter is applied in order to soften the data array. Next, it is expanded to the dimensions of the original matrix, replicating it until it becomes in an *NxM* matrix, defined as Filter Matrix (FM) in

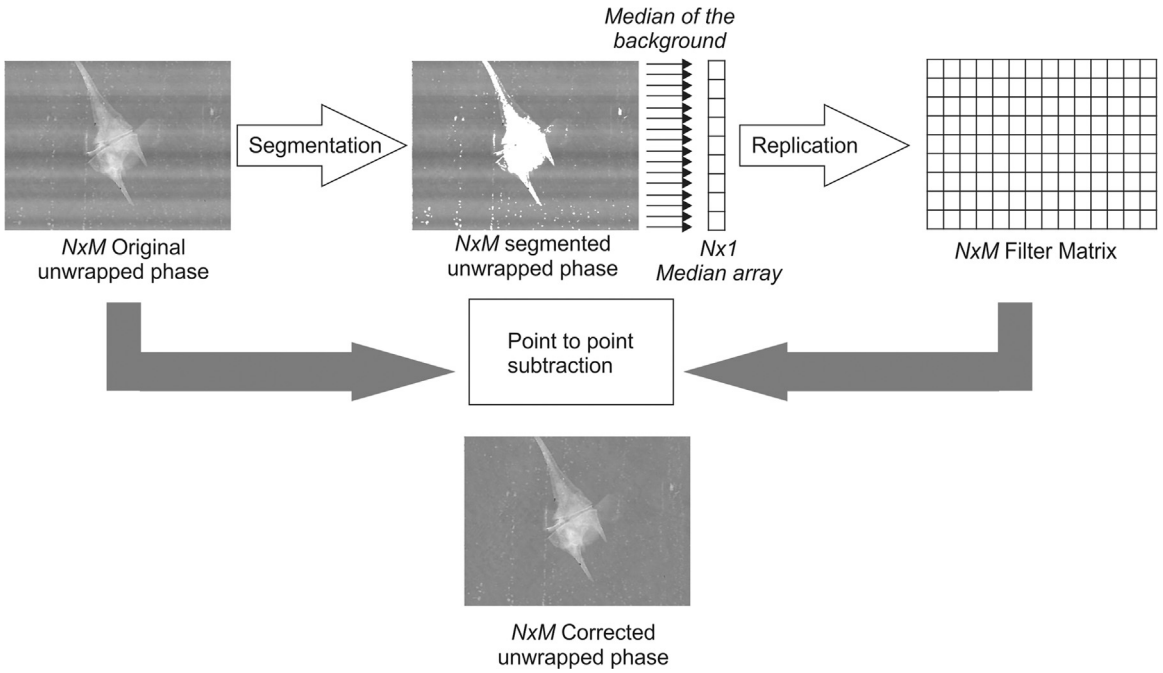

Fig. 4. RSE correction procedure.

the context of this paper. Finally, the FM is subtracted point by point from the original unwrapped phase matrix.

It is worth to emphasize that, in order to calculate the median of the background data of each row a segmentation procedure is required. The segmentation method must exclude any phase values of the object under study or any background pixels that have values of the order of phase delays introduced by the object. Thus, the segmentation is performed row by row, discarding the set of pixels whose phase values deviates in average above a target value. In this regard, a binary search algorithm was chosen, using as "target value" the mean STD of several arrays extracted for the background of the unwrapped phase. The whole methodology for correcting RSE aberration is summarized in Fig. 4.

Finally, the choice of the median, as a representative value of the RSE, over the mean average is justified inasmuch as the median is an actual phase value and, unlike the mean average, outliers do not affect it. As a consequence, the methodology proposed does not affect phase values in a relevant way as it will be discussed in the next section.

4. Results and discussion

In our experiment, both the camera and the object are static during the readout process while the interference fringes, resulting from superposition of the reference wave with the object wave, may oscillate or vibrate due to external factors. Therefore, the RSE affects only the phase and it is not reflected in the amplitude. Due to the fact that in applications like DHM, the relevant information is encoded in the phase, all aberrations resulting from the experimental devices or environmental disturbances should be corrected before relating it with the physical quantity to be measured.

Applying the algorithm described above, the FM of the spurious fringes introduced by RSE is calculated and subtracted point by point from the original unwrapped phase. As a result, a phase map, free of spurious ripples, is obtained as it can be seen in Fig. 5(c). The FM is also shown in Fig. 5(b), conveniently transformed into gray levels for illustration.

Once the RSE was corrected, the STD of an area of the image background was calculated yielding a value of 0.17. This value can be considered as a typical phase error introduced by holographic imaging, which is susceptible to various sources of noise, including quantization noise, shot noise, thermal noise, vibrations and sometimes even speckle [14]. Accordingly, aberration introduced by RSE has been compensated.

The experiment described above has been carried out under vibration isolation conditions, essential in holography. In order to estimate phase error introduced by the RSE under non-vibration isolated environment, a hologram without object was registered soon after hitting vigorously the holographic table.

Assuming no air temperature variations, the refractive index of the sample, irrespective of the external vibrations, is supposed to be uniform over the entire field of view so that the phase should be approximately constant. Hence, theoretically, it is expected that hologram fringes are straights and parallels. On the contrary, the hologram exhibits fringes highly distorted by the RSE, as depicted in the inset of Fig. 6(a). The obtained unwrapped phase maps, with and without applying the proposed method to correct the RSE are shown in Fig. 6(b) and (c) respectively. In this case, due to the highly unstable conditions, it is evident that the uncorrected unwrapped phase is extremely corrupted by the RSE. However, despite some remaining artifacts, a reduction of RSE aberrations is very noticeable in the corrected phase map.

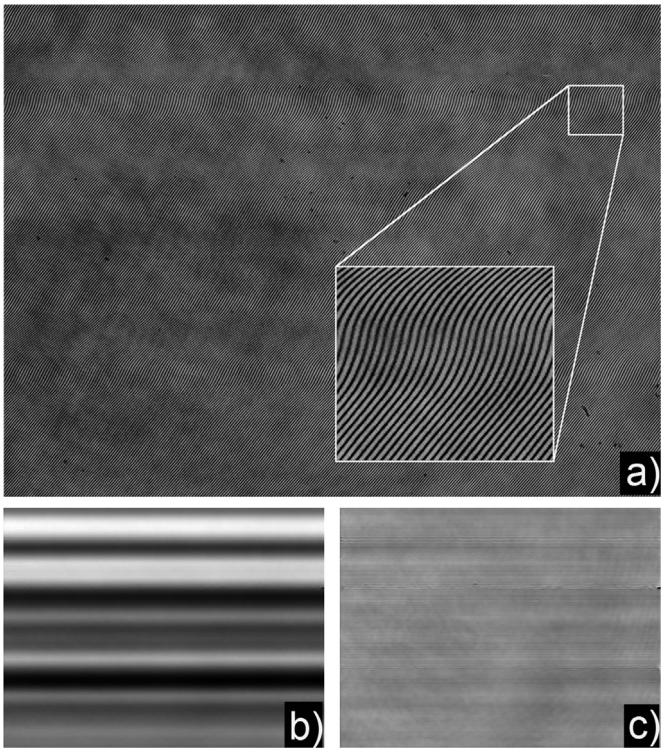

Fig. 6. : a) Hologram after hitting the table. b) Unwrapped phase map. c) Corrected unwrapped phase map.

To assess phase variations introduced by the RSE, from the phase contrast images of Fig. 6(b) and (c), several line profiles, horizontal (X) and vertical (*Y*) were analyzed. As an example, data obtained for a test row and a test column with and without correction are compared in Fig. 7(a) and (b) respectively.

As expected, the phase variations in the horizontal direction for both, the non-corrected (Test row uncorrected) and corrected (Test row corrected) phase map, are similar with a STD of 0.26 and 0.21 respectively (equivalent to optical path lengths ~26 nm and 21 nm). However, in the vertical direction, variations in the

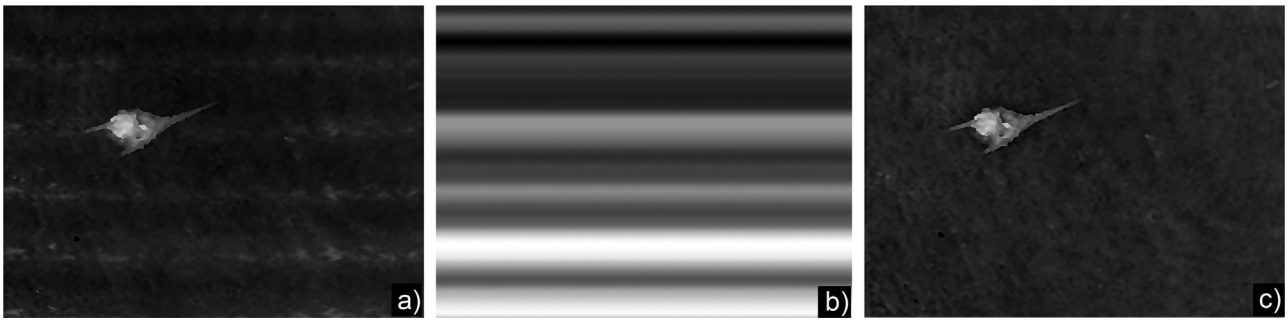

Fig. 5. : a) Original unwrapped phase map, b) Filter Matrix, c) Corrected unwrapped phase map.

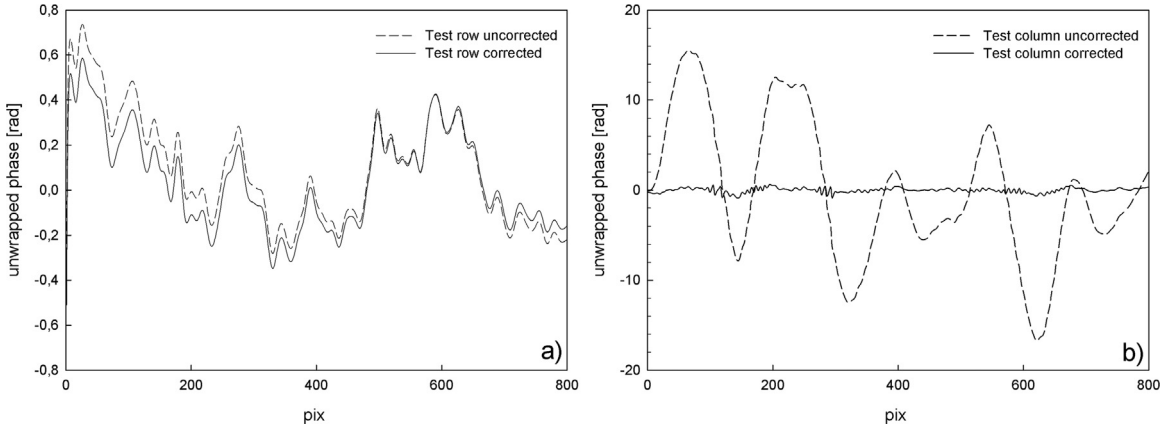

Fig. 7. Line profiles of phase contrast image a) *X*-profiles. b) *Y*-profiles.

uncorrected phase map (Test column uncorrected) are much more significant, with a STD of 7.5. Thus, in these conditions, the RSE introduces a noise level equivalent to an optical path length ~759 nm, giving rise to multiple 2π phase steps. If no correction is performed, the information of an object under study will be masked by the RSE. Furthermore, in DHM applications, where microscopic objects are analyzed, errors introduced by RSE could seriously affect the accuracy of measurements. Correction of RSE results in a STD for the test column of 0.26 (Test column corrected), a value 28 times smaller than that obtained for the uncorrected test column, and consistent with the test row phase noise. This means that our methodology corrects properly phase errors introduced by rolling shutter effect even under extremely non-vibration isolated environment.

5. Conclusions

A fast and simple method for correcting phase aberrations introduced by rolling shutter effect typical from CMOS sensors is presented. To our knowledge, there are no reports for correcting this effect for interferometric applications. Results show that this effect can be corrected easily, which could encourage the replacement of expensive CCDs in Digital Holographic Microscopy.

The proposed algorithm, due the nature of image processing tools used, preserves the actual pixels values of the images almost unaltered. Their effect on the relevant phase information is negligible even in extremely non-vibration isolated environment. The simplicity of the method encourages the use of a low-cost CMOS camera in an application like Digital Holographic Microscopy for those who already have a rolling shutter CMOS camera in their labs and are unwilling to or financially cannot afford a new latest version with global shutter technology incorporated, thereby preventing unwanted rolling shutter effect on images of moving objects.

Acknowledgments

The authors acknowledge the valuable collaboration of Miss J. Passamai in reviewing the English writing. This work was supported by ANPCyT-PME, 1392/2 and Research Council of the National University of Salta, Project no. 2161.

References

[1] M. Jacquot, P. Sandoz, G. Tribillon, High resolution digital holography, Opt. Commun. 190 (2001) 87–94.
[2] C.-K. Liang, Y.C. Peng, H. Chen, Rolling shutter distortion correction, in: Proceedings of the SPIE (The International Society for Optics and Photonics), Beijing, China, 2005, pp 59603V-59603V-8.
[3] O. Ait-Aider, A. Bartoli, N. Andreff, Kinematics from Lines in a Single Rolling Shutter Image, in: Proceedings of the IEEE (Institute of Electrical and Electronics Engineers), Minneapolis, MN, USA, 2007, pp 1–6.
[4] C.-K. Liang, L.-W. Chang, H.H. Chen, Analysis and compensation of rolling shutter effect, IEEE (Inst. Electr. Electron. Eng.) 17 (2008) 1323–1330.
[5] U. Schnars, W.O. Jueptner, Digital Holography. Digital Hologram Recording, Numerical Reconstruction and Related Techniques, Springer-Verlag, Berlin Heidelberg, Germany, 2005.
[6] E. Cuche, P. Marquet, C. Depeursinge, Simultaneous amplitude-contrast and quantitative phase-contrast microscopy by numerical reconstruction of Fresnel off-axis holograms, Appl. Opt. 38 (1999) 6994–7001.
[7] L. Yu, M. Kim, Wavelength-scanning digital interference holography for tomography three-dimensional by use of the angular spectrum method, Opt. Lett. 30 (2005) 2092–2094.
[8] F. Palacios, J. Ricardo, D. Palacios, E. Gonçalves, J.L. Valin, R. De Souza, 3D image reconstruction of transparent microscopic object using digital holography, Opt. Commun. 248 (2005) 41–50.
[9] C.J. Mann, L. Yu, C. Lo, M.K. Kim, High-resolution quantitative phase-contrast microscopy by digital holography, Opt. Express 13 (2005) 8693–8698.
[10] J.-B. Chun, H. Jung, C.-M. Kyung, Suppressing rolling-shutter distortion of CMOS image sensors by motion vector detection, IEEE (Inst. Electr. Electron. Eng.) 54 (2008) 1479–1487.
[11] A.C. Monaldi, G.G. Romero, E.E. Alanís, C.M. Cabrera, Digital Holographic Microscopy for microalgae biovolume assessment, Opt. Commun. 336 (2015) 255–261.
[12] J.W. Goodman, Introduction to Fourier Optics, second ed., Mc Graw-Hill Companies, Inc., USA, 1996.
[13] C.J. Mann, P.R. Bingham, H.K. Lin, V.C. Paquit, S.S. Gleason, Dual modality live cell imaging with multiple-wavelength digital holography and epi-fluorecence, 3D Research 2 (1) (2011) 1–6, eid 5.
[14] N. Pandey, B. Hennelly, Effect of additive noise on phase measurement in digital holographic Microscopy, 3D Research 2 (1) (2011) 1–6, eid 6.